ELSEVIER

Chemical Geology 206 (2004) 97–118

CHEMICAL GEOLOGY
INCLUDING
ISOTOPE GEOSCIENCE

www.elsevier.com/locate/chemgeo

Rare earth elements, yttrium and Pb isotope ratios in thermal spring and well waters of West Anatolia, Turkey: a hydrochemical study of their origin

P. Möller[a,*], P. Dulski[a], Y. Savascin[b], M. Conrad[a]

[a] *GeoForschungsZentrum Potsdam, PB 4.3 Lagerstattenbildung, Telegrafenberg A-50, D-14473 Potsdam, Germany*
[b] *Dokuz Eylul University, Geothermal Energ. Rese. a. App. Center, Izmir, Turkey*

Received 27 March 2003; accepted 23 January 2004

Abstract

Rare earth elements (REE), yttrium, major elements and Pb isotope ratios were determined in thermal well and spring waters, and rocks of the Büyük Menderes and Gediz grabens, Turkey, which includes the geothermal fields of Kizildere, Salavatli, Germencik, Kula and Salihli. Together with the results of short- and long-time leaching of local rocks, REE and Y and Pb isotope ratios indicate that the Palaeozoic mica schists dominantly control the REE and Y signatures of the deep-seated Na–HCO_3 waters. Marbles may also be involved, but their low REE contribution is overridden by the much higher REE and Y abundances in the mica schists. Palaeozoic gneisses can be excluded as source rocks by both Pb isotope ratios and REE leaching behaviour. The deep-seated waters either ascend rapidly in production wells and precipitate carbonate-silica scales at temperatures of about 200 °C or these waters ascend slowly to springs, become enriched in Ca^{2+}, Cl^- and SO_4^{2-}, and discharge with temperatures up to 100 °C as fumaroles or hot springs. Some of these spring waters precipitate large amounts of travertine upon exsolution of CO_2. In contrast, the thermal Ca–HCO_3-type of water from Pamukkale has its source in the regional Pliocene limestones.

Keywords: Rare earth elements; Yttrium; Spring water; Geothermal waters; Geothermal fields; Hydrochemistry; Kizildere; Turkey

1. Introduction

In the last 25 years, the distribution of rare earth elements (REE) has been studied in black smoker vent fluids (Klinkhammer et al., 1994; James et al., 1995), in dispersed flows at the ocean floor (Michard et al., 1993), in fumaroles (Michard, 1989; Honda et al., 1989a,b; Lepel et al., 1989; Kikawada et al., 1993; Aggarwal et al., 1996; Lewis et al., 1998; Middlesworth and Wood, 1998; Möller et al., 2003), and in thermal spring waters (Michard and Albarede, 1986; Möller et al., 1998; Möller, 2000). All these fluids represent the results of water–rock interactions under various temperatures, total pressures, and CO_2 partial pressures. In general, these fluids differ from those of their host rocks in REE abundance and trends of REE patterns. REE abundance in fluids is mainly controlled by leachable accessory minerals, REE exchange with rock-forming minerals and their amorphous surface coatings, and coprecipitation of REE with alteration

* Corresponding author. Tel.: +49-331-2881430; fax: +49-331-2881436.
E-mail address: pemoe@gfz-potsdam.de (P. Möller).

0009-2541/$ - see front matter © 2004 Elsevier B.V. All rights reserved.
doi:10.1016/j.chemgeo.2004.01.009

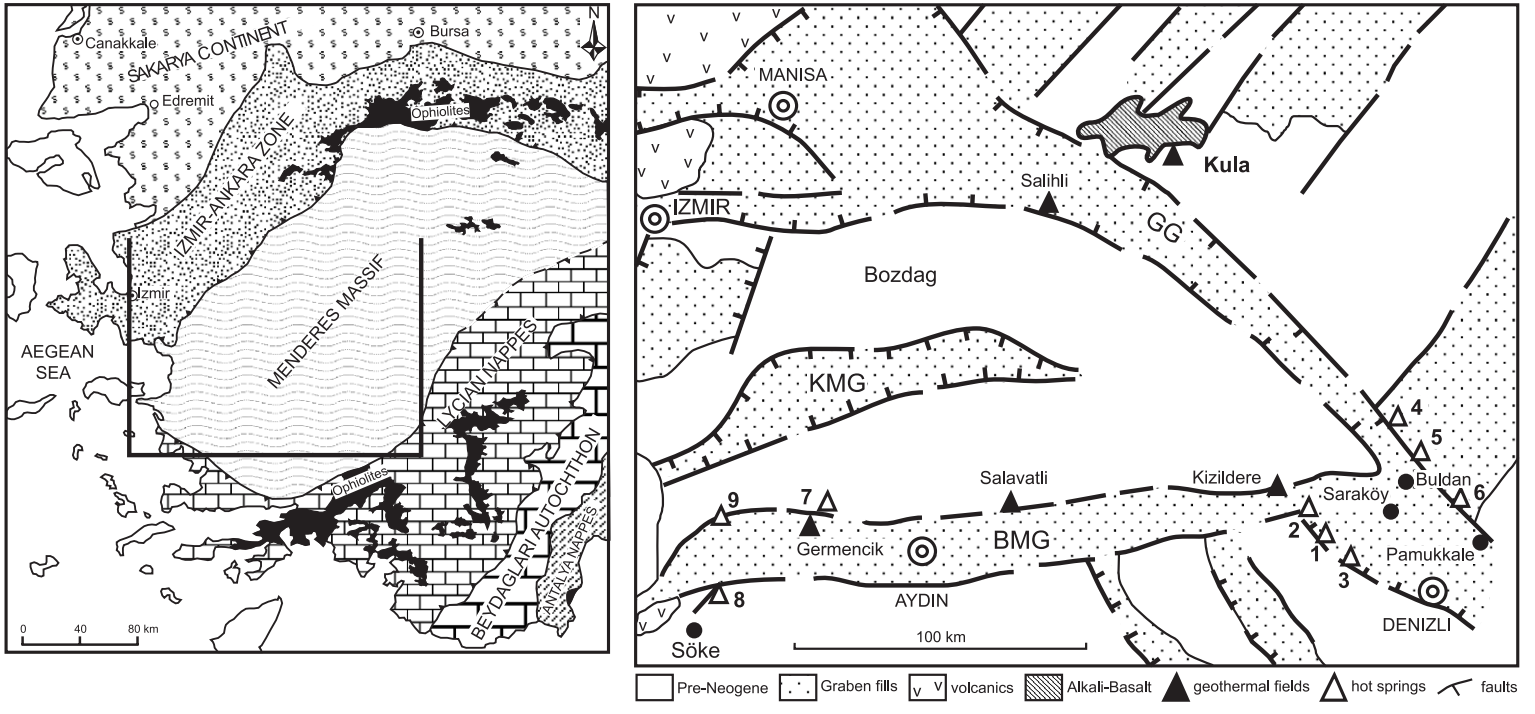

Fig. 1. Palaeo-neotectonic rock assemblage of south-western Turkey (modified after Okay et al., 1991). The blown-up rectangular of the overview shows the details of the neotectonic framework and the major grabens of south-western Turkey. The geothermal fields of Salavatli, Germencik, Kizildere, Salihli and Kula are given by solid triangles. The wells (open triangles) are numerated according to Table 1. GG = Gediz Graben; BMG = Büyük Menderes Graben; KG = Küyük Menderes Graben.

minerals (Möller, 2002). Leaching experiments on possible source rocks of waters indicate that REE and Y (hitherto combined to REY) strongly depend on the degree of rock alteration (Irber, 1996; Möller and Giese, 1997; Giese and Bau, 1994; Möller, 2002).

The fractionation of REY and especially the anomalous behaviour of Ce, Eu and Y in aqueous systems has been studied in great detail. Bau (1999) and Kawabe et al. (1999) discussed the Y–Ho fractionation and defined the Y anomaly as the normalised Y/Ho ratio. Anomalous Y develops in aqueous systems because Y is less adsorbed onto mineral surfaces. Ce is easily oxidised when scavenged by FeOOH (Bau, 1999; Kawabe et al., 1999). Therefore, all oxygen-rich waters acquire a negative Ce anomaly (Bau and Dulski, 1996; Möller, 2002; Möller et al., 2003). Eu behaves anomalously partly because of its reduction to Eu(II) at temperatures above 250 °C (Sverjensky, 1984; Bilal, 1991; Bau and Möller, 1992). Like Y, Eu(II) is less adsorbed onto mineral surfaces and, thus, moves faster with migrating waters than the other trivalent REE (Möller, 1998). Anomalies, however, can also be inherited from water–rock interaction. For instance, negative Ce anomalies can be inherited from marine limestone, if it is poor in clay minerals (Parekh et al., 1977). Negative Eu anomalies are mostly inherited from felsic rocks (Möller, 2002), especially from granites because of chloritisation of biotite with its tiny solid inclusions showing strongly negative Eu anomalies (Möller et al., 1985; Möller, 2002).

This contribution focuses on the REY abundance in thermal spring and well waters from a geothermally active region of West Anatolia, Turkey (Fig. 1a), where fluids of 30 to 200 °C were sampled. The main objectives of this study are: Which rock units are involved in water–rock interaction and establish the observed REY abundance in the waters? Are the thermal spring waters related to the deep-seated aquifers with high-temperature water, or do they originate from different sources?

2. Geological settings

The most prominent geodynamic factor of the study area is the northerly directed subduction of the African plate underneath the Greek and Anatolian plate along the Cyprus–Hellenic subduction zone. This has induced extensional features in Greece, the Agean Sea, and western Anatolia. The hanging-wall plate overthrusts the subducting slab at different velocities, a process which is still active today (Doglioni et al., 2002). The post-orogenic extension is responsible for the geological situation of W Anatolia, where coexisting lacustrine sediments and coeval volcanic rocks unconformably overly metamorphic rocks, ophiolitic nappes and flysch sediments of the basement (Fig. 1a). From NW to SE Anatolia, the pre-Neogene is part of the tectonic units of the western Pontides (Sakarya Continent; Sengör, 1979), the collisional Izmir–Ankara Zone, the Menderes Massif, and the tectonic units of the western Taurids, which are covered by Cenozoic sedimentary and volcanic rock successions.

The Menderes Massif is the oldest rock assemblage of the Anatolian Continent and comprises high-grade gneisses and schists overlain by low-grade schist, marble, phyllite, metaplutonites and metasedimentary rocks associated with recrystallised limestones. The main metamorphism occurred between Late Cretaceous and Early Miocene (Erdogan and Güngor, 1992). The Miocene metasedimentary rocks are succeeded by mega-sequences of clastic, carbonate- and organic-rich sedimentary rocks (Fig. 2), deposited as alluvial fans, fluvial carbonate mudflats and ephemeral shallow freshwater carbonate lake deposits. Volcanic facies and borate deposits interfinger these sedimentary sequences. The Pliocene sedimentary succession resembles that of the underlying Miocene in composition.

As a result of the Bozdag uplift, grabens developed to the N and S of the Bozdag Horst (Fig. 1b). Due to rapid uplift, high seismicity, and erosion, very thick and coarse-grained alluvial and fluvial Pliocene–Quaternary sediments accumulated in the Gediz, Kücük Menderes, and Büyük Menderes grabens. These grabens are more or less E–W trending with depressions or basins formed by the NE–SW to NW–SE directed extensions.

In W Anatolia, the shoshonitic and ultrapotassic–lamproitic association of the Early–Middle Miocene calc-alkaline volcanism is considered to be related to the oceanic subduction that developed in the Aegean area after the Cretaceous–Eocene collision of the Sakarya and Anatolian continents (Francalanci et al., 2000). The second alkaline volcanic phase started in the Middle Miocene and increased volumetrically

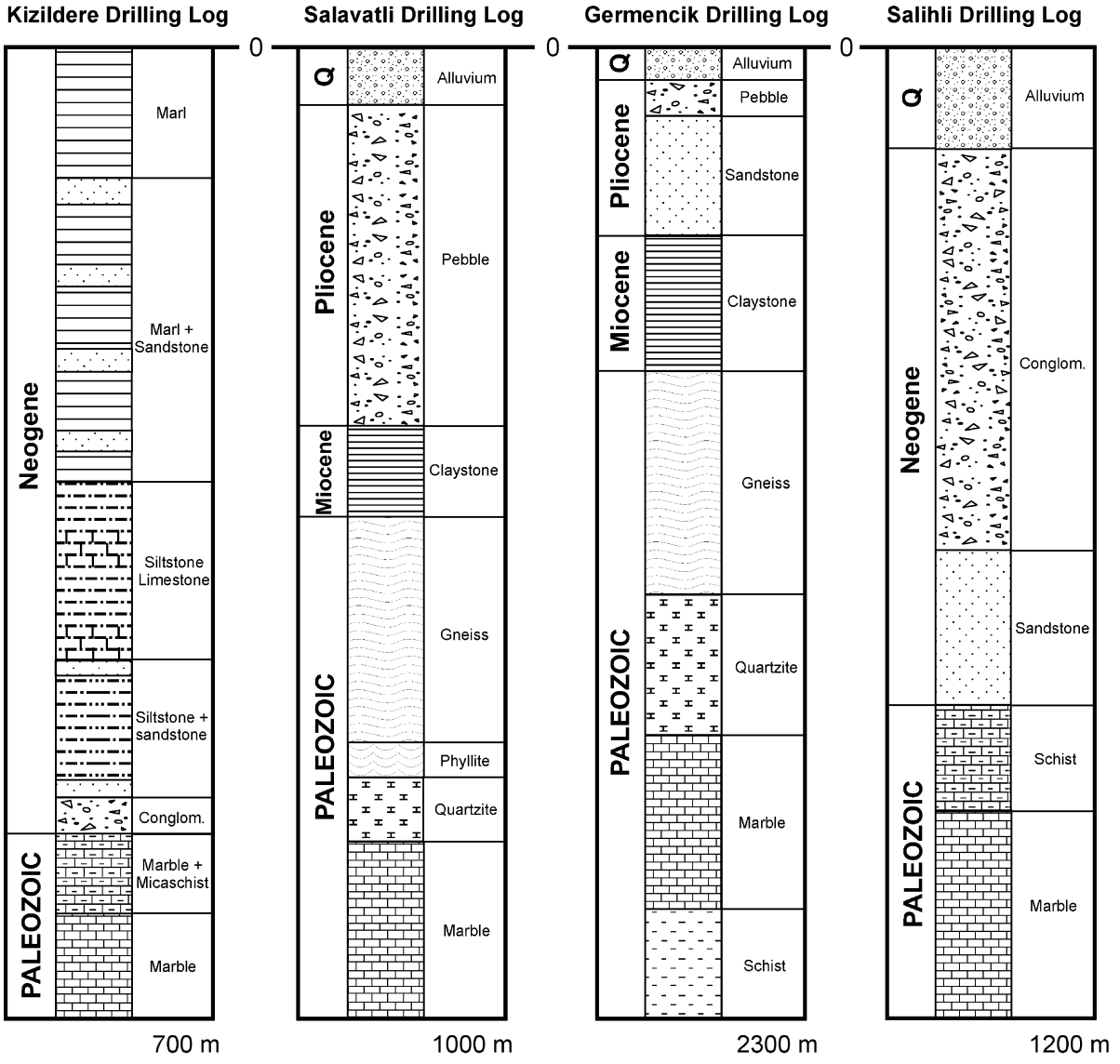

Fig. 2. Simplified drilling logs for geothermal fields of Kizildere, Salavatli, Gemencik, and Salihli.

with time. It became dominant beyond the Upper Miocene. The younger trachybasaltic–basaltic vulcanites and ultrapotassic–lamproidic rocks result from the intra-continental extensional tectonics (Doglioni et al., 2002; Innocenti et al., in press). In contrast to the widely distributed former calc-alkaline strato-type volcanics, the younger alkaline rock assemblages occur as small dykes and domes within the grabens. One of the typically calc-alkaline to shoshonitic volcanic centres is located near Söke in the Büyük Menderes Graben (Fig. 1b).

2.1. The geothermal fields

Most of the geothermal systems are related to intersections of the youngest E–W trending grabens and older NW–SE and NE–SW striking faults (Fig. 1b). The Kizildere Geothermal Field is part of the

enormous Denizli–Buldan–Sarayköy geothermal area near to the junction of the Gediz and the Büyük Menderes Graben (Fig. 1b). At the geothermal plant of Kizildere, eight wells, cased to depths of 500 to 1000 m, produce extremely CO_2-rich fluids from the crystalline basement (Fig. 2) with bottom hole temperatures up to 240 °C and pressures ranging from 50 to 90 bar. Under bottom hole conditions, the fluids contain about 0.2 to 0.4 mol of dissolved CO_2 per kg fluid (Satman et al., 1999). The exsolution of CO_2 starts at approximately 500 m below surface and a Sr-rich carbonate scale, initially aragonite, precipitates together with silica. Numerous thermal springs occur in the Kizildere Geothermal Field. The hot spas of Tekkehamam, Babacik, and Ujuzhamami are located at the southern flank of the Büyük Menderes Graben. The hot spas of Gölemezli, Yenice, Pamukkale are situated at the eastern flank of the Gediz Graben.

The Salavatli Geothermal Field is located at the scarp of the northern main border fault of the Büyük Menderes Graben (Fig. 1b). Two wells were drilled in 1982 down to 1510- and 962-m depth into the basement (Fig. 2) yielding artesian water of 167 and 172 °C, respectively.

The tectonic and stratigraphical features at Germencik are quite similar to those at Salavatli (Fig. 2). The

Table 1
Sampling localities and characterisation of sampled waters

Geothermal fields	Description	Depth, m	Bottom hole temperature, °C	Salinity, mg/kg	Eh, mV (SHE)
Kizildere	Geothermal power plant 20 MW; liquid-CO_2 production plant; eight wells in operation with a total output of 1200 tons/h	250–1100	200–240	3400–4400	−8 to −116
Germencik	Exploration wells	1000–2400	200–230	4200–6000	−150–+30
Salavatli	Exploration wells	1500; 960	240	4400	
Salihli	Production wells for hot spa Kursunlu	962–1510	200–240	2100	−150 to −190
Kula	Exploration well, CO_2-rich water;	160	106	4600	0
	Fokurdak hot pool;		98	4100	240
	Spring on top of travertine ridge;		96	4300	60
	Mineral water well at bottling plant		73	3550	380
Thermal springs and wells	**Description**	**Depth, m**	**Outflow temperature, °C**	**Salinity**	**Eh, mV (SHE)**
Tekkehamam; 1 in Fig. 1b	Several springs; pool with carbonate mud, CO_2 emanating; bath, hot spa	–	72	3000	−70
Babacik; 2 in Fig. 1b	Spring used in hot spa, H_2S; CO_2 emanating	–	60	2700	<−20
Ujuzhamami; 3 in Fig. 1b	Hot pool, hot spa	–	variable	4000	<35
Yenice; 4 in Fig. 1b	Reddish spring water in bath because of FeOOH colloids;	–	20–40	3100	200–300
	Spring on travertine ridge; Fe poor,	–	25–50	3700	180
	Well no. 3, water supplied to hot spa	not known	50		24
Gölemezli; 5 in Fig. 1b	Several springs, hot spa	–	40–50	4300	
Pamukkale; 6 in Fig. 1b	CO_2 emanating springs in pools of Pamukkale Hotel and of the police station, (Jandarma)	–	20–40	2700	360–430
Bozköy; 7 in Fig. 1b	Artesian well, water supplied to hot spa	160	50–65	5200	<0
Sazliköy; 8 in Fig. 1b	Spring; hot spa	–	25	1800	200
Gümüsköy; 9 in Fig. 1b	Well water supplied to hot spa	31	40	2600	20–340

Table 2
Chemical composition of waters

	Kizildere															
	KD6 96/30	KD6 97/10	KD6 98/20	KD6 99/13	KD13 97/06	KD13 98/01	KD13 99/06	KD14 98/16	KD15 97/16	KD15 98/05	KD15 99/26	KD16 96/21	KD16 96/22	KD16 98/10	KD16 99/21	KD21 98/13
T	~ 190	~ 190	~ 190	~ 190	~ 190	~ 190	~ 190	~ 190	~ 190	~ 190	~ 190	~ 190	~ 190	~ 190	~ 190	~ 190
pH	6.71	6.33	6.64	6.8	6.41	6.49	6.8	7.11	6.55	6.23	6.15	6.8	6.85	6.54	6.9	6.27
Eh				− 43			− 82				− 23				− 116	
Na	43.04	55.4	45	43.2	42.4	48.2	44.4	49.8	41.6	46	40.7	46.3	46.3	50.5	47.4	48.8
Li	0.53	0.68	0.53		0.69	0.55		0.56	0.69	0.52		0.62	0.62	0.57		0.55
K	2.72	1.67	2.81	3.22	2.59	2.94	4.7	3.35	2.66	2.83	2.94	3.16	3.16	3.25	3.79	2.94
Ca	0.083	0.029	0.027	0.058	0.024	0.073	0.06	0.023	0.025	0.051	0.052	0.033	0.033	0.029	0.044	0.037
Mg				0.029			0.018				0.008				0.008	
Cl	2.55	4.01	3.35	2.22	3.92	3.52	2.21	5.11	4.55	3.61	2.15	2.93	2.93	3.98	2.46	3.84
HCO_3	37.3	34.6	38.9	35.6	34.9	39.0	41.2	40.9	35.6	36.7	32.5	38.9	38.9	40.7	39.5	42.9
F				0.69			0.75				0.87				1.001	
SO_4				6.2			6.05				6.78				6.39	
Y	3.49	1.90	0.51	0.76	1.17	0.90	2.15	1.73	0.73	0.54	1.62	5.62	3.21	1.82	1.18	3.00
La	2.34	2.43			1.40		1.37				3.13	4.29		1.17		0.86
Ce	5.55	5.79			3.60		6.36	1.77	2.78		6.77	6.20	3.55	1.96		3.24
Pr	0.68	0.67	0.16		0.36	0.10	0.51	0.22	0.30	0.07	0.81	0.69	0.45	0.15		0.30
Nd	2.27	2.11	0.51		1.30	0.34	1.32	0.79	0.95	0.20	1.33	2.88	1.72	0.53		1.02
Sm	0.46	0.23	0.09	0.10	0.22	0.08	0.25	0.15	0.18	0.06	0.21	0.51	0.31	0.10	0.17	0.23
Eu			0.02	0.02		0.02	0.04				0.04			0.02	0.04	0.04
Gd	0.28	0.19	0.08	0.10	0.14	0.06	0.20	0.14	0.13	0.06	0.16	0.55	0.32	0.18	0.15	0.25
Tb				0.02			0.03				0.02			0.02	0.03	0.04
Dy	0.35	0.17	0.08	0.12	0.16	0.07	0.27	0.21	0.12	0.07	0.25	0.57	0.31	0.15	0.23	0.24
Ho		0.03	0.01	0.01		0.02	0.04			0.01	0.02	0.09		0.02	0.03	0.05
Er	0.18	0.10	0.03	0.04	0.06	0.04	0.11			0.03	0.07	0.26	0.16	0.07	0.06	0.13
Yb		0.09	0.02	0.03		0.04	0.09			0.03	0.06	0.25		0.06	0.05	0.12
Lu				0.01			0.01				0.01			0.01	0.01	0.01
Y/Ho		34	27	32		31	32			27	36	33		44	23	34
206/208	0.479	0.471	0.466	0.483	0.484	0.473	0.483	0.474	0.474	0.472	0.469	0.471	0.470	0.474	0.484	0.470
207/208	0.416	0.394	0.403	0.404	0.419	0.411	0.404	0.403	0.411	0.416	0.395	0.410	0.409	0.409	0.408	0.405
206/207	1.15	1.20	1.16	1.19	1.16	1.15	1.19	1.17	1.15	1.13	1.19	1.15	1.15	1.16	1.19	1.16

The major ion contents are given in mmol/kg, whereas the rare earth elements and Y are given in pmol/kg. No values are given when either not measured or, in case of REY, the necessary corrections exceeded 30% of the initial intensities of REY in ICP-MS measurements. The Pb isotope ratios are a by-product of ICP-MS measurements with a precision of about ±1% (Möller et al., 1998). Y/Ho ratios are given in g/g.

Table 2 (*continued*)

Kizildere				Germencik									Salavatli	Salihli	
KD21 99/17	KD22 98/18	KD22 99/09	Average	ÖB1 96/14	ÖB1 97/32	ÖB3 97/33	ÖB3 98/34	ÖB6 97/34	ÖB6 98/35	ÖB9 96/15	ÖB9 97/35	ÖB9 98/33	2 96/43	1 95/27	2 95/28
~ 190	~ 190	~ 190	~ 190	203	203	230	230	221	221	211	211	211		94	97
6.27	5.35	6.3	6.5	6.07	5.97	6.7		6.4		8.33	6.22		8.44	7.28	7.86
− 49		− 8	− 53		16	− 125		− 99			− 93		50		
40.3	40.7	41.8	45.3			69.7							45.8		
	0.48		0.584			1.5							0.78		
2.84	2.63	3.2	3.021			4.2							2.1		
0.049	0.032	0.046	0.043			0.2							0.82		
0.01		0.008	0.014												
1.93	3.30	2.06	3.191			7.0							6.82		
34	34.5	41.1	37.8			70							46.7		
0.8		0.73	0.807												
5.82		5.69	6.15			0.7							1.24		
1.70	10.53	3.49	2.42	400	260	300	179	275	4723	1815	884	17.0	153.5	4.62	11.31
2.17	1.32	2.13	2.06	235	99.8	176	78.8	57	701	775	264	7.1	50.2	3.63	9.35
6.63	6.07	4.70	4.64	371	217	387	156	118	2380	1649	519	15.7	136	6.49	13.24
0.90	0.77	0.56	0.453	44	26.2	48.4	17.5	17.1	358	213	68.8	1.88	17.4	0.56	0.91
1.14	2.37	1.39	1.30	161	97.5	180	62.7	68.5	1447	838	266	7.10	59.1	1.80	2.74
0.14	0.51	0.27	0.224	27	18.2	41.3	13.2	19.2	399	218	63.2	1.77	16.8	0.28	0.64
0.02	0.11	0.07	0.039	3.1	2.9	11.4	5.7	21.2	421	35	21.3	0.61	2.6	0.09	0.21
0.08	0.57	0.27	0.206	30			15.3		441	242		1.99	16.6	0.31	0.89
0.02	0.11	0.04	0.036	4.2	3.0	6.0	2.2	3.7	67	38	12.5	0.26	2.9	0.04	0.11
0.14	0.73	0.32	0.241	24	17.8	32.5	12.8	22.1	375	209	78.2	1.47	16.9	0.36	0.54
0.02	0.16	0.06	0.041	5.1	3.6	5.9	2.4	4.1	68	40	15.6	0.28	3.3	0.06	0.07
0.07	0.50	0.16	0.122	15	9.9	14.0	6.7	11.0	178	106	43.7	0.67	9.8	0.18	0.14
0.07	0.53	0.13	0.112	12	8.0	8.6	5.6	8.7	152	83	38.5	0.49	10.4	0.46	0.08
0.01	0.08	0.02	0.018	1.8	1.2	1.1	0.8	1.2	22	12.4	5.3	0.07	1.6	0.02	0.003
38	35	34	32	42	39	28	40	36	38	24	31	33	25	43	90
0.471	0.466	0.463	0.474	0.476	0.481	0.468	0.472	0.484	0.486	0.496	0.484	0.465	0.462	0.474	0.479
0.407	0.403	0.406	0.407	0.418	0.446	0.401	0.402	0.412	0.395	0.412	0.415	0.385	0.409	0.410	0.417
1.16	1.16	1.14	1.16	1.14	1.08	1.17	1.17	1.18	1.23	1.21	1.16	1.21	1.13	1.16	1.15

(continued on next page)

Table 2 (*continued*)

	Tekkehamam		Babacik				Ujuzhamami		Gölemezli			Yenice					
	pool 95/5	Hamam 98/28	spring 95/7	spring 96/36	spring 97/03	spring 98/27	pool 95/8	pool 98/29	well 95/1	well 95/2	well 96/40	bath 96/38	bath 97/29	bath 98/24	crest 96/39	crest 97/30	well 3 98/25
T	73	70	58	59	60	54	70	55.5	50	50	38	23	38	36	26	50	52.3
pH	7.1	7.8	6.12	6.2	6.45	6.25	6.85	7.57	6.13	6.1	6.32	6.44	6.27	6.22	6.74	6.4	6.59
Eh	− 88	− 56	H2S	H2S	− 17	− 77	H2S	35			100		300	217		180	24
Na	35				22.3			51			23.6		12.1			24.2	
Li	0.3				0.26			0.68			0.26		0.07			0.05	
K	3.4				3.51			3.1			1.6		6.7			4.45	
Ca	1.95				6.1			0.29			9.8		7.4			7.1	
Mg	0.58				3.5			0.02			5.6		1.7			1.7	
Cl	2.6				2.54			3			2.68		1.12			1.6	
HCO_3	5.7				7.5			15.7			11		11.5			15.3	
F	0.53				0.26			0.6			0.12		0.13			0.17	
SO_4	15.3				12.7			10.5			17		3.4			7.4	
Y	31.7	18.0	123	159	99.1	81.9	476	260	103	105	92.7	>13,000	14,776	13,670	281	444	2448
La	10.0	1.11	50.0	69.7	11.8	3.9	167	56	27.2	22.6	8.9	918	436	160	5.5	4.4	2
Ce	26.9	9.09	95.0	184.8	58.6	31.1	329	150	55.6	49.36	34.44	1456	1301	779	12.0	20.7	15
Pr	2.86	1.20	9.3	20.5	7.1	4.35	39	18	5.38	4.62	3.38	255	229	174	2.0	3.0	5
Nd	10.2	5.68	35.1	76.1	28.0	19.38	145	68	19.82	17.57	13.57	1164	1058	914	9.6	13.8	35
Sm	2.15	1.70	6.8	14.9	6.1	5.55	31	15	4.24	3.70	3.08	367	330	337	3.0	5.1	32
Eu	0.45	0.44	1.5	3.2	1.4	1.37	7.1	3.8	0.90	0.82	0.81	120	110	111	1.0	1.9	12
Gd	2.72	2.36	8.3	15.8		7.15	35	18	5.27	5.11	5.06	696		682	8.1		84
Tb	0.37	0.37	1.3	2.4	1.1	1.07	5.7	3	0.89	0.87	0.81	138	127	130	1.4	2.7	16
Dy	2.67	2.34	8.0	14.0	7.1	6.76	37	20	6.18	5.72	5.73	961	951	941	10.9	21.7	129
Ho	0.48	0.45	1.6	2.7	1.4	1.36	7.6	4.5	1.37	1.34	1.28	221	218	211	2.9	5.2	30
Er	1.38	1.18	4.8	7.6	4.2	3.88	23	14	4.21	4.17	4.10	654	643	639	10.3	16.7	93
Yb	1.18	0.90	3.6	5.9	3.0	3.01	21	14	3.55	3.65	3.40	543	540	542	11.3	14.9	80
Lu	0.16	0.13	0.5	0.9	0.4	0.43	2.9	2.00	0.52	0.53	0.54	76	76	74	2.0	2.1	11
Y/Ho	36	22	41	32	37	32	34	31	41	42	39		37	35	53	46	44
206/208	0.477	0.454	0.467	0.479	0.469	0.476	0.470	0.477	0.467	0.465	0.460	0.457	0.465	0.467	0.474	0.492	0.466
207/208	0.406	0.398	0.411	0.406	0.414	0.416	0.410	0.401	0.410	0.410	0.408	0.392	0.398	0.410	0.407	0.424	0.407
206/207	1.17	1.14	1.14	1.18	1.13	1.14	1.15	1.19	1.14	1.13	1.13	1.17	1.17	1.14	1.16	1.16	1.15

Table 2 (*continued*)

Kula				Sazliköy	Gümüsköy			Bosköy		Pamukkale					
well 99/03	ridge 99/04	Forkudak 99/02	filling pl. 99/01	spring 96/10	well 96/11	well 98/31	Hamam 98/32	well 96/12	well 96/13	Hotel 95/4	Hotel 97/28	Jandarma 96/42	Jandarma 97/26	Jandarma 98/26	Jandarma 99/29
57.4	56.00	34.2	18.7	24.3	42	41.5	39.3	61.6	49.1	35	37	23	37	32	33.00
6.84	6.69	6.54	6.25	6.3	6.2	6.2	6.45	6.45	6.5	6.1	6.24	6.19	6.16	6.14	6.15
3	58	236	376			20	339	H2S	H2S		427		410	370	
41	41.4	37.6	16.3								1.7				
											0.02				
2	2.2	1.8	1.1								3.5				
2	1.5	2.6	7.5								11.8				
4	3.4	4.0	5.1								4				
5	5.1	3.5	3.1								0.6				
50	43.0	46.4	39.7								9				
0.14	0.14	0.15	0.05								0.08				
1	1.27	1.7	0.32								11.3				
123	5	4688	3713	1261	507	485	416	494	764	1427	1379	1274	1337.4	1190	1252
4.71	7.32	53.1	28	169	33.9	16.8	16.8	25.7	18.5	181.4	49.7	90.3	40.9	17.5	26.43
22.20	17.60	153	25	396	52.3	37.9	36.8	51.1	31.2	91.8	17.1	19.6	13.5	8.0	13.52
4.08	2.11	72.9	19	41.6	6.8	5.5	5.4	7.9	5.2	40.3	34.3	31.8	31.0	18.1	25.26
17.50	5.72	387	99	175	32.5	27.1	25.0	35.5	27.7	175.8	159.8	142.6	146.1	99.1	126
4.32	0.92	138	28	39.7	9.4	8.2	6.2	10.9	9.9	36.9	38.3	33.9	35.6	34.4	32.39
1.52	0.17	44	13	10.4	3.3	3.1	2.0	3.6	5.4	9.8	10.6	9.5	9.9	9.5	8.95
5.90	0.80	243	67	58.8	28.3	26.3	11.8	19.4	27.1	54.3		51.6		52.8	48.7
1.00	0.11	43	13	9.7	5.6	5.3	2.2	4.0	4.9	8.3	8.8	7.8	8.2	7.9	7.42
7.02	0.57	309	109	66.3	44.6	42.6	16.7	29.0	34.8	56.2	59.6	53.1	56.3	51.6	50.9
1.62	0.10	71	31	15.5	10.3	9.8	4.2	6.9	8.1	12.7	13.4	12.5	12.6	12.0	11.55
5.30	0.25	209	111	47.2	26.9	25.8	14.0	20.8	24.0	38.3	38.7	36.4	37.2	34.8	34.14
6.19	0.17	174	129	43.4	15.5	15.2	13.2	18.7	22.3	27.0	27.5	25.7	26.9	25.1	24.96
1.01	0.02	26	22	6.6	1.8	1.8	1.9	2.7	3.4	3.7	3.9	3.6	3.8	3.5	3.36
41	26	36	64	44	26	27	53	39	51	60	55	55	57	54	58
0.485	0.494	0.464	0.466	0.465	0.476	0.462	0.467	0.467	0.476	0.500	0.473	0.471	0.467	0.466	0.462
0.397	0.406	0.414	0.411	0.415	0.409	0.420	0.407	0.404	0.409	0.398	0.393	0.408	0.396	0.410	0.405
1.22	1.22	1.12	1.13	1.12	1.16	1.10	1.15	1.16	1.16	1.26	1.20	1.16	1.18	1.14	1.14

bottom hole temperatures are as high as 231 °C and the reservoir rocks are similar to those at Kizildere. The associated thermal springs of this area are those of the hot spas of Bosköy, Sazliköy and Gümüsköy.

Four exploration wells have been drilled in the Salihli Geothermal Field through the Miocene–Pliocene conglomerate, sandstone, mudstone, limestone and tuff into the Paleozoic schists, quartz schists, micaschists and marbles of the Menderes Massif (Fig. 2). The thermal water is supplied to spas.

The Kula geothermal field is located on a block of crystalline rocks (Fig. 1b). As the youngest volcanics of Western Anatolia, the Kula volcanics are Na-dominant in character, while all the former volcanic series of Western Anatolia are K-dominant rocks. About 1 km to the west of the spa, a sparkling thermal water is bottled as mineral water.

2.2. Sampling

The sampling locations of thermal waters together with their salinity, redox potential (Eh), and temperature are given in Table 1. The waters above 100 °C were sampled at the well heads by leading the water through a stainless steel spiral for cooling by fresh water (Möller et al., 2003). The cooling system was connected to the production pipe by a metal-mantled rubber tube. The fluid was depressurised to 1 bar during sampling. The quenched fluid only lost its non-condensable gas fraction (mainly CO_2) together with about 1% of water as part of the vapour phase at about 30 °C. Although the water/steam ratio of the sampled fluid was not constant with time, a sampling time of about 30 min was expected to yield a reliable average. Eh and pH were measured in the water at about 30 °C. Whenever possible, thermal springs were sampled by introducing a silicon tube into the outlet as deep as possible.

At each locality, 5 to 10 l of waters were filtered (0.2 μm Sartobran®, Sartorius, Germany) as soon as possible by means of a peristaltic pump. The filtrate was spiked with 1 ml of a 100 ng/g Tm solution. All waters were adjusted to pH 2 by addition of 6 M sub-boiled HCl. Because the sample treatment was done in the field, all possible precautions had to be taken to prevent dust from entering the system (Möller et al., 2003). At each sampling site, 60-ml samples of filtered water were collected for anion and cation determinations.

Rock samples were collected from outcrops in the countryside of Kizildere, Kula and Pamukkale. Travertine is ubiquitous at springs, the most impressive ones are the white terraces of Pamukkale. Carbonate-silica scales were collected from piles in the pilot plant of Kizildere. The samples represent scales from the well casing (about 200 °C), the separator (140 °C), and the effluents of the silencers (about 90 °C).

2.3. Analytical methods

2.3.1. Major elements in water

Li^+, Na^+, K^+, Mg^{2+}, Ca^{2+}, F^-, and S (mainly SO_4^{2-} because H_2S was negligible) were determined by inductively coupled plasma atomic emission spectrometry (ICP-AES) using matrix-adjusted standard solutions for calibration prepared from single standard element solutions (Tirisol®, Merck, Germany). Reproducibility of measurements was better than ± 5%. Cl^- was titrated in the untreated water by $AgNO_3$ with a precision of ± 4%. The concentrations of HCO_3^- of the sampled fluids have been estimated from titration against of 6 M HCl, when adjusting the waters to about pH 2 as needed in the preconcentration procedure of REY (Möller et al., 2003). The accuracy of the derived HCO_3^- concentration is within ± 10%. Borate and sulphide species do not interfere with the applied calculation of HCO_3^- contents at sub-neutral values, and their contents are low. The redox potential (Eh) was determined at the wellhead by using a calibrated Pt electrode (Mettler Toledo InLab 505) with an internal Ag/AgCl reference electrode. The results are referenced to the standard hydrogen electrode (SHE). All analytical data of waters are compiled in Table 2.

2.3.2. REY

Two to ten hours after adjustment to pH 2, the waters were passed through preconditioned SepPakC_{18}® cartridges (Water, USA) containing an adsorbate comprising a mixture of different ethylhexylphosphates (Merck) acting as a liquid cation exchanger. The cartridges were enclosed in parafilm for storage and transportation. In the laboratory, the cartridges from the field loaded with REY were washed with 50 ml 0.01 M sub-boiled HCl, and the REY were eluted with 40 ml 6 M sub-boiled HCl at a rate of 3 ml/min. After

Table 3
Chemical composition of rocks and scale

	Kizildere Geothermal Field										Kula area			Pamukkale area			
	Gneiss	Quartzite	Schist+marble		Limestone	Shale	Travertine	Scale at 145 °C	Scale at >190 °C	Scale at >90 °C	Basalt	Marble	Mica schist	Vein calcite	Marl	Limestone	Travertine
Sample numbers	2	1	3	1	2	4	1	8	5	2	1	1	1	3	1	3	1
Carbonate content, %	0	0	19	62	97	20	100	95	96	85	1	100	1	100	93	97	100
Dimension	μg/g	μg/g	μg/g	μg/g	μg/g	μg/g	μg/g	ng/g	ng/g	ng/g	μg/g	μg/g	μg/g	μg/g	μg/g	μg/g	μg/g
Y [μg/g]	38.5	8.7	16.7	9.6	48.3	37.7	5.72	2.90	5.19	13.41	23.48	3.06	22.69	17.04	1.88	4.31	3.23
La	9.8	13.5	24.5	7.3	21.9	41.8	5.50	5.09	9.73	15.14	50.56	1.57	29.84	3.89	2.20	1.98	5.36
Ce	22.9	29.2	47.0	11.1	48.2	85.5	14.71	10.38	18.52	36.65	89.96	0.76	60.82	7.53	4.22	2.93	10.19
Pr	2.8	3.4	5.6	1.6	5.8	10.1	2.27	1.28	2.03	4.36	9.79	0.24	7.38	1.25	0.54	0.53	1.19
Nd	11.0	11.7	19.7	6.1	20.1	35.8	9.21	4.61	7.05	15.82	36.37	0.88	28.17	5.29	2.06	2.33	4.06
Sm	3.58	2.37	3.64	1.23	4.81	6.88	1.98	0.88	1.16	3.00	6.65	0.17	5.53	1.46	0.44	0.50	0.76
Eu	0.51	0.34	0.79	0.47	0.39	1.39	0.43	0.25	0.28	0.54	2.13	0.04	1.17	0.39	0.10	0.12	0.16
Gd	4.67	2.01	3.35	1.23	5.65	6.72	1.97	0.73	0.98	2.55	5.83	0.21	4.77	2.01	0.41	0.55	0.73
Tb	0.99	0.33	0.51	0.19	1.17	1.07	0.26	0.10	0.15	0.38	0.82	0.03	0.71	0.35	0.06	0.08	0.10
Dy	6.91	1.84	2.99	1.19	8.17	6.72	1.33	0.54	0.87	2.25	4.63	0.23	4.20	2.37	0.34	0.52	0.60
Ho	1.44	0.33	0.59	0.26	1.72	1.42	0.23	0.10	0.17	0.43	0.86	0.05	0.81	0.51	0.06	0.11	0.12
Er	4.52	0.88	1.70	0.73	5.21	4.18	0.55	0.27	0.48	1.20	2.40	0.17	2.42	1.53	0.17	0.34	0.35
Tm	0.72	0.14	0.26	0.10	0.81	0.63	0.07				0.33	0.02	0.35	0.23	0.12	0.12	0.05
Yb	4.65	0.95	1.65	0.60	5.04	4.03	0.39	0.21	0.40	1.04	2.11	0.16	2.27	1.44	0.14	0.32	0.37
Lu	0.64	0.14	0.25	0.09	0.66	0.58	0.05	0.03	0.06	0.14	0.31	0.03	0.33	0.21	0.02	0.05	0.05
Pb	9.2	2.1	15.4	8.2	2.1	14.8								0.5	–	1.2	–
Th	19.1	7.8	9.0	0.7	29.7	14.2								1	4.8	0.54	4.1
U	3.6	5.9	0.9	4.2	4.0	2.8								1	0.2	0.75	1.7
Y/Ho [g/g]	27	27	29	38	28	27	24	29	31	32	27	58	28	33	30	39	26
Pb (206/208)	0.622	0.529	0.476	0.485	0.572	0.474					0.479	0.483	0.473				
Pb (207/208)	0.376	0.388	0.399	0.399	0.345	0.399					0.403	0.398	0.402				
Pb (206/207)	1.66	1.36	1.19	1.22	1.69	1.19					1.19	1.22	1.18				

Figures in parentheses indicate the number of analyses average. All analyses are given in (μg/g).

Table 4
Leachates of various rocks from the study area

	Palaeozoic rocks and their leachates															Tertiary rocks and their leachates					
	Gneiss						Schist + marble									Shale					
	91	91 1 h	91 20 h	*92*	92 1 h	92 20 h	*58*	58 1 h	58 20 h	*5*	5 1 h	5 20 h	*60*	60 1 h	60 20 h	*50*	50 1 h	50 20 h	*62*	62 1 h	62 20 h
La [μg/g]	*9.8*	0.6	0.9	*9.7*	0.5	1.0	*24.8*	1.2	1.6	*7.29*	0.63	1.1	*28.2*	1.1	1.7	*35.6*	0.4	1.61	*71.7*	1.0	2.4
Ce	*23.0*	1.4	2.5	*22.8*	1.2	2.6	*46.4*	2.4	3.4	*11.13*	1.1	1.8	*55.5*	2.2	4.0	*74.4*	1.1	4.38	*146.6*	2.2	5.7
Pr	*2.8*	0.22	0.36	*2.8*	0.21	0.39	*5.8*	0.31	0.5	*1.57*	0.18	0.26	*6.6*	0.3	0.5	*8.6*	0.2	0.64	*17.4*	0.3	0.8
Nd	*10.9*	0.93	1.50	*11.1*	0.9	1.6	*20.2*	1.2	1.8	*6.06*	0.77	0.99	*22.9*	1.0	2.1	*29.3*	0.6	2.51	*62.9*	1.1	3.2
Sm	*3.5*	0.34	0.52	*3.6*	0.33	0.56	*3.7*	0.26	0.38	*1.23*	0.17	0.21	*4.2*	0.22	0.48	*6.3*	0.2	0.62	*12.4*	0.2	0.7
Eu	*0.5*	0.05	0.08	*0.5*	0.05	0.08	*0.9*	0.06	0.09	*0.47*	0.07	0.08	*0.9*	0.05	0.11	*0.63*	0.02	0.06	*2.41*	0.05	0.14
Gd	*4.6*	0.45	0.70	*4.7*	0.44	0.73	*3.3*	0.27	0.38	*1.23*	0.19	0.22	*4.0*	0.25	0.49	*6.1*	0.13	0.56	*11.0*	0.21	0.64
Tb	*0.98*	0.085	0.131	*1.00*	0.083	0.139	*0.46*	0.04	0.05	*0.19*	0.03	0.034	*0.64*	0.040	0.074	*1.10*	0.02	0.09	*1.6*	0.03	0.08
Dy	*6.84*	0.53	0.80	*6.97*	0.52	0.85	*2.6*	0.25	0.28	*1.19*	0.19	0.21	*3.98*	0.25	0.42	*7.4*	0.11	0.53	*8.8*	0.11	0.38
Y	*38.9*	2.4	3.6	*38.1*	2.2	3.8	*15.9*	1.7	1.8	*9.63*	1.5	1.7	*21.1*	1.3	2.0	*48.9*	0.53	2.58	*43.2*	0.37	1.28
Ho	*1.45*	0.10	0.15	*1.44*	0.09	0.16	*0.5*	0.05	0.06	*0.26*	0.04	0.04	*0.79*	0.05	0.08	*1.64*	0.02	0.10	*1.6*	0.02	0.05
Er	*4.50*	0.25	0.40	*4.55*	0.24	0.41	*1.6*	0.17	0.18	*0.73*	0.12	0.13	*2.13*	0.13	0.20	*5.05*	0.06	0.27	*4.5*	0.03	0.11
Tm	*0.71*	0.03	0.05	*0.72*	0.03	0.05	*0.22*	0.03	0.03	*0.10*	0.02	0.02	*0.29*	0.02	0.03	*0.76*	0.01	0.04	*0.6*	0.00	0.01
Yb	*4.62*	0.20	0.31	*4.68*	0.18	0.32	*1.5*	0.20	0.21	*0.60*	0.10	0.11	*1.87*	0.10	0.15	*5.01*	0.06	0.22	*4.0*	0.02	0.06
Lu	*0.60*	0.02	0.04	*0.60*	0.02	0.04	*0.2*	0.03	0.03	*0.09*	0.01	0.02	*0.27*	0.01	0.02	*0.70*	0.01	0.03	*0.6*	0.00	0.01
Pb	*3.16*	0.28	0.56	*2.96*	0.27	0.50	*18.1*	0.7	1.4	*8.17*	1.1	1.2	*10.75*	0.26	0.69	*3.08*	0.03	0.11	*12.2*	0.04	0.16
Th	*9.24*	0.07	0.12	*9.13*	0.07	0.12	*8.2*	0.05	0.04	*0.71*	0.01	0.02	*11.31*	0.02	0.04	*3.14*	0.01	0.06	*22.5*	0.04	0.1
U	*19.2*	0.24	0.32	*19.1*	0.22	0.32	*0.58*	0.02	0.03	*4.16*	0.20	0.21	*1.2*	0.02	0.04	*27.6*	0.06	0.16	*1.5*	0.02	0.0
Y/Ho [g/g]	*26.8*	23.9	24.4	*26.5*	24.3	24.7	*30.4*	31.5	31.2	*37.5*	37.7	37.5	*26.8*	27.4	25.7	*29.8*	24.9	25.8	*26.3*	23.7	24.1
Pb (206/208)	*0.613*	0.860	0.818	*0.630*	0.877	0.849	*0.474*	0.479	0.470	*0.485*	0.484	0.483	*0.473*	0.473	0.479	*0.573*	0.518	0.555	*0.486*	0.464	0.478
Pb (207/208)	*0.378*	0.393	0.391	*0.388*	0.391	0.390	*0.396*	0.399	0.395	*0.399*	0.402	0.399	*0.390*	0.394	0.401	*0.374*	0.394	0.378	*0.400*	0.381	0.404
Pb (206/207)	*1.62*	2.19	2.09	*1.62*	2.25	2.17	*1.20*	1.20	1.19	*1.22*	1.20	1.21	*1.21*	1.20	1.20	*1.53*	1.31	1.47	*1.21*	1.22	1.18

The REY content of the leachates after 1 and 20 h are given in μg/g of the original rock. The Pb isotope ratios are a by-product of ICP-MS measurements and are precise within ± 1% only (Möller et al., 1998). The composition of the whole rock is given in *italics*.

evaporation to dryness, the residues were taken up by 1 ml of 5 M sub-boiled HNO_3. These solutions were spiked by a Ru–Re mixture for possible corrections of the internal shift of the response factors in inductively coupled plasma mass spectrometry (ICP-MS) measurements if necessary (Bau and Dulski, 1996) and filled up to 10 ml with purified water. Details of the measurements are given by Dulski (2001). Calibration solutions were prepared from single element standard solutions (CertiPUR® ICP standards (Merck) traceable to SRM from NIST). Several corrections were necessary because of interferences of molecular ions with the desired mono-charged ions of the REE (Dulski, 1994). Blank corrections for La, Ce, and Pr, which are contaminants of the commercially available liquid cation exchanger (Merck), were necessary. Additionally, due to enhanced Sb contents of the waters, $^{139}La^{+}$ had to be corrected for $^{123}Sb^{16}O^{+}$ (Möller et al., 2003). The accuracy of the heavy REE is better than ± 5%, whereas that of the light REE is variable depending on the degree of necessary corrections. If they exceeded 30% of the measured intensities, data are not given in Table 2. As a by-product of ICP-MS measurements, $^{206}Pb/^{208}Pb$, $^{207}Pb/^{208}Pb$, and $^{206}Pb/^{207}Pb$ isotope ratios were also determined by ICP-MS with reproducibility of about ± 1% (Möller et al., 1998).

2.3.3. Whole rocks and scales

Powdered whole rocks from outcrops (0.1 g) were digested by a 1:1 mixture of HF and $HClO_4$ at 170 °C under vapour saturation conditions. The acidic solutions were evaporated to incipient dryness, the residue dissolved in 1 ml of concentrated HCl and diluted to 50 ml. To aliquots of 1 ml of sample solution, 0.1 ml 1 μg/g Re and Ru spike solutions were added for drift corrections and filled up to 10 ml. In these solutions, REY were determined by ICP-MS (Dulski, 2001) applying the standardisation as described above. The results are given in Table 3.

Dried and powered carbonate-silica scales of 1 to 5 g were treated with in 6 M sub-boiled HCl. The insoluble residue was separated by 0.2 μm cellulose acetate filter (Sartorius) and the dissolved fraction was determined by subtracting the mass of the dried residue from the original weight. The filtrates were diluted to 4 l by Milli Q water and the highly acidic solutions were adjusted to pH 2 by adding ultra-pure NH_4OH (Merck). This dilution was necessary because Ca^{2+} at concentrations exceeding 0.1 mol/kg starts replacing the light REE on the cartridge. This procedure was necessary in order to get rid of the high salt content and to enrich REY for measurements by ICP-MS. The determination of REY followed the procedure described for water samples. The analytical results are given as REY abundance of the carbonate fraction (Table 3).

2.3.4. Leachates

In order to determine the easily leachable fractions of REY, aliquots of ground rock powders (0.5 g) were mixed with ion exchange resin loaded with H^{+} ions (4 g) and 50 ml of supra-pure water. Several batches of this mixture were shaken for 1 and 20 h. After the elapsed time, rock powder and resin were separated by wet sieving. The resin was eluted by 40 ml of sub-boiled 6 M HNO_3. Aliquots of the eluate were diluted with Milli-Q water and REY were measured by ICP-MS (Table 4). The detailed leaching procedure and the interpretation of the leaching results are discussed in Möller and Giese (1997).

3. Results

3.1. Rocks and scales

The analysed rocks of the Kizildere and Kula areas (Table 3) show REY patterns with rather similar trends and negative Eu anomalies, excepting the Kula basalt (Fig. 3a). Among the Paleozoic rocks, the gneisses are lower in LREE and show more negative Eu anomalies than the mica schists. The REY patterns of the Pliocene shales and limestones resemble the Palaeozoic mica schists. The Tertiary limestones of the Kizildere and Pamukkale areas and the Palaeozoic Kula marble are the lowest in REY of the studied rocks. The Kula marble differs from the Tertiary limestones by both strong negative Ce and positive Y anomalies. The REY abundance of the ubiquitous travertines (Fig. 3b) is similar in to those of the local limestones (Fig. 3a). The REY patterns of the various high-temperature carbonate scales from Kizildere show very low REY abundances and rarely anomalies.

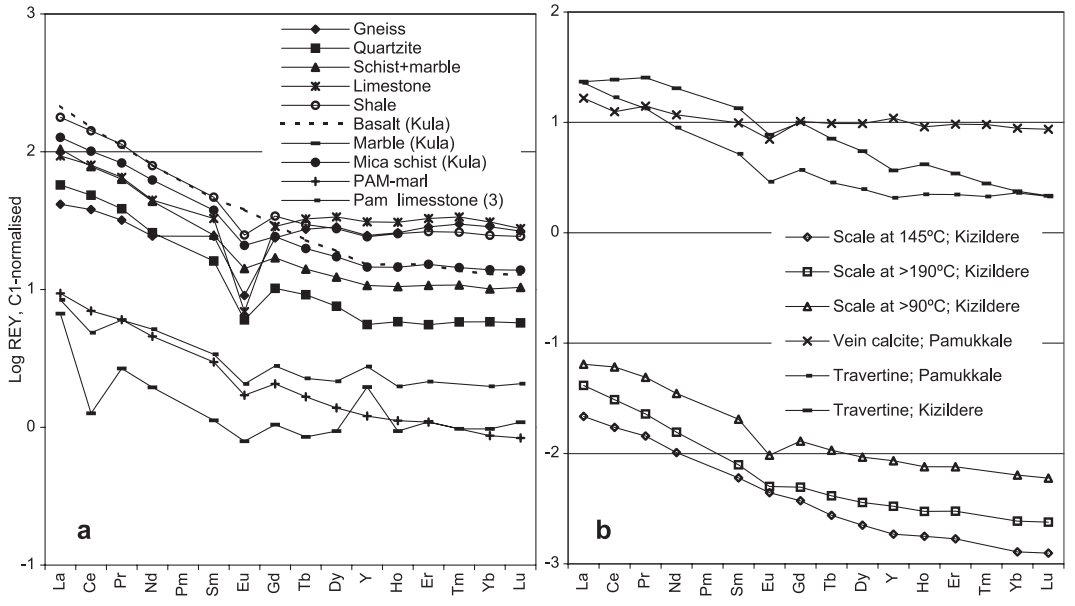

Fig. 3. Chondrite-normalised REY patterns of local aquifer rocks, travertines, and scales. (a) The REY patterns are subparallel and split into two groups. The REY patterns of siliceous rocks differ from those of the limestones and marble. (b) The carbonate scales from the production pipes and silencers of Kizildere differ significantly in REY abundance from travertines and vein calcites from limestones near Pamukkale.

3.2. Leachates

Source-rock-normalised REY abundances of the leachates after 1 and 20 h are shown in Fig. 4a and b, respectively. Comparison of leachates of the same rock evidences that leached REY abundances not only increase with time but they are also fractionated. Two types of REY patterns of leachates occur: (i) convex trends characterise gneisses and Pliocene shales, and (ii) trends steadily increasing from La to Lu without any significant anomalies are typical for mica schist.

3.3. Major elements in water

The analysed waters widely differ in major element composition (Table 2). In the Langelier and Ludwig (1942) diagram, all high-temperature waters (>100 °C) with salinities ranging from 2100 to 6400 mg/kg (Table 1) plot narrowly together (KIZ in Fig. 5). The Ca and Mg contents are the lowest in the area. These waters are chemically reducing ($-190 < Eh < -10$ mV), sometimes with a slight H_2S odour, and they precipitate carbonate scales upon CO_2 exsolution.

The spring waters with salinities ranging from 1800 to 5200 mg/kg (Table 1) widely scatter in chemical composition (Table 2). The chemical variations are not related to Eh or temperature. Compared with Kizildere water, this Na–HCO_3 type of water is low in CO_2 contents but shows enhanced in Ca^{2+} and Mg^{2+} contents. High sulphate contents occur in Tekkehaman, Babacik, Ujuzhamami, and Gölemezli, which may partly be due to H_2S oxidation in the course of mixing with influent oxygen-rich water. The waters of Gümüsköy, Bosköy, ÖB1, and ÖB9 are highest in Na^+ and Cl^-. The Pamukkale water is of the Ca–HCO_3 type. The Pamukkale waters (33 °C) and the Kula mineral water (19 °C) have high Eh values in common (Table 2).

3.4. REY in water

The C1-chondrite-normalised REY patterns of the reported waters cover five orders of magnitude (Figs. 6 and 7). They can be subdivided into four groups according to their patterns (Table 5). The *first group* comprises the high-tempertaure (>100 °C), CO_2-rich water-steam systems of Kizildere, Salavatli, Germencik (ÖB samples), and Salihli. Regionally associated are the thermal springs of Tekkehamam, Babacik, Ujuzhamami, Gölemezli and Sazliköy. Water samples

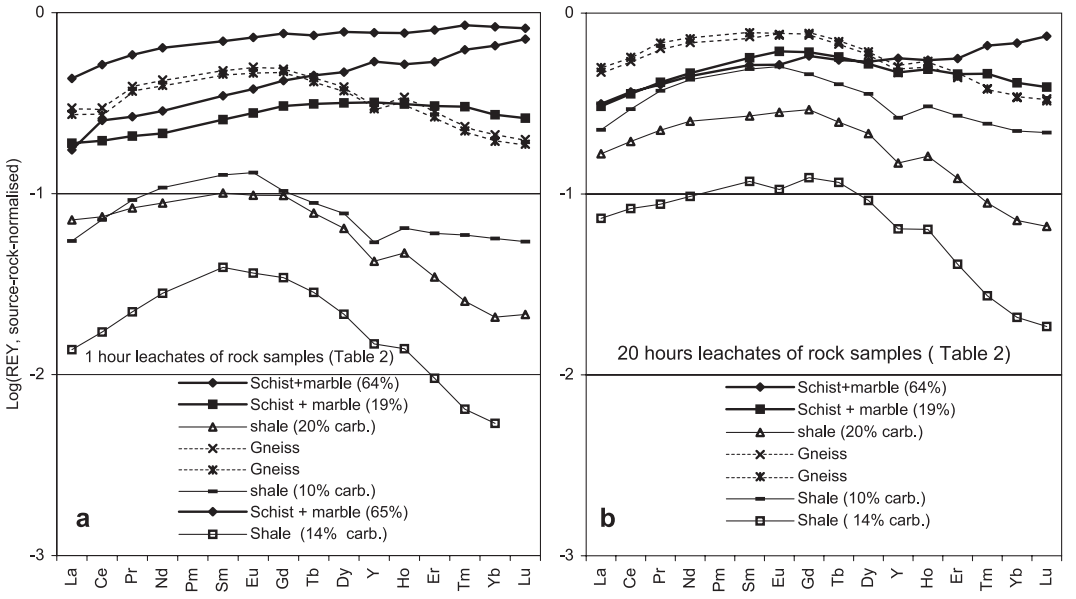

Fig. 4. The source-rock normalised REY patterns of the 1- and 20-h leachates are quite similar. The time of leaching controls the abundance of REY but not the type of pattern. Fractionation of REY occurs during leaching as evidenced by different trends of REY patterns after 1- and 20-h leaching.

from Kizildere, repeatedly collected over 4 years and from different wells (Table 2), are presented by thin lines without symbols in Fig. 6a. The spread of this field is attributed to real changes in the REY abundances in the water (Middlesworth and Wood, 1998) and not to irreproducible sampling and/or preconcentration procedure as shown by the good reproducibility of repeated analyses of water from Yenice-bath (Fig. 7a) and Pamukkale (Fig. 7d). All REY patterns of the high-temperature waters decrease from La to Lu but the REY abundance of the waters from the exploration wells of Gemencik and Salavatli is much higher than in those of the high-flow production wells of Kizildere. The Kizildere waters show no anomalous Y behaviour, which indicates that the source rocks are leached under steady state conditions (Möller et al., 2003). In contrast, the water from Salihli with its marked Y anomaly indicates that steady state is not yet reached. The negative Eu anomalies of the waters are inherited from the source rocks (Fig. 3a). Excepting Eu, the REY patterns of scale carbonates from the production pipes resemble the patterns of the water, thereby indicating that REY fractionation in the fluid is negligible at high temperatures. The REY patterns of the thermal springs at Gölemezli, Tekkehamam, Babacik, Ujuzhamami, and Sazliköy show inherited negative Eu and achieved positive Y anomalies (Fig. 6b). These patterns resemble those of the Kizildere waters.

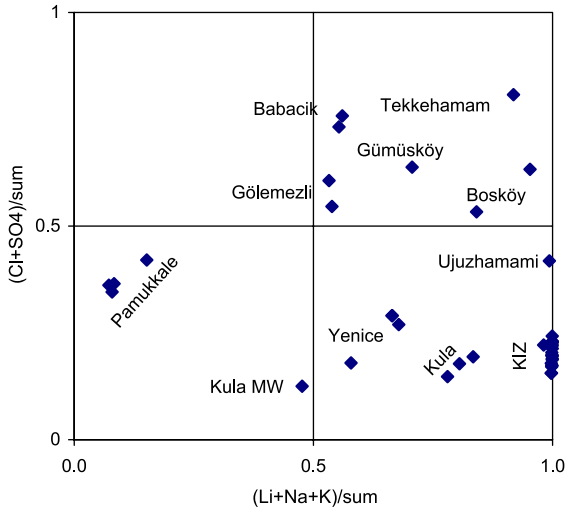

Fig. 5. Langelier and Ludwig (1942) diagram of the studied waters. The deep waters of Kizildere, Salavatly, Germencik and Salahli plot closely together (KIZ), whereas most of the spring waters scatter over three quadrants because of their enhanced Ca/Na- and HCO_3/($Cl + SO_4$) equivalent ratios compared to KIZ group. Kula MW = Kula mineral water (MW).

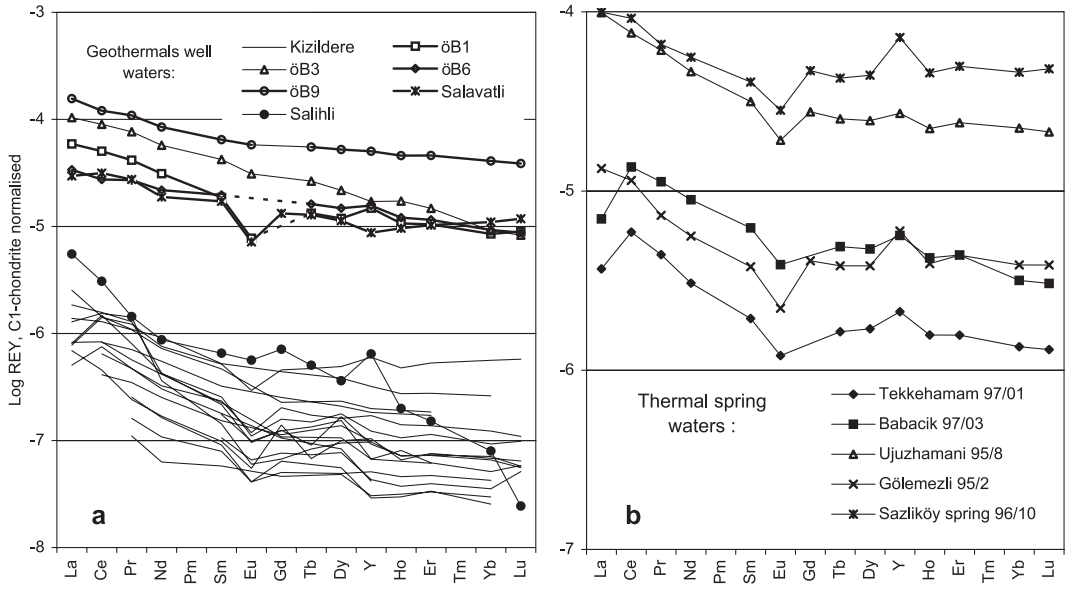

Fig. 6. C1-chondrite-normalised REY patterns of the various types of waters. (a) Well head fluids from Kizildere (19 water analyses of 7 wells sampled during 4 years), Salihli (average of two samples), Germencik (each of the ÖB-well patterns represents averages of two samples), and Salavatli; (b) geothermal spring waters in the surroundings of Kizildere and Söke.

The *second group* (Table 5) comprises REY patterns of the thermal waters of Yenice (Fig. 7a), Bosköy and Gümüsköy (Fig. 7c). Normalised heavy REY are higher than the light. The Yenice spring water feeding the bath shows enhanced REY abundance because of FeOOH colloids (Eh about +220 mV), which stain the water deep red. The Yenice well water increases from light to heavy REE resulting in a trend which is steeper than that of the local spring (Fig. 7a).

At Kula (Fig. 7b), waters from the well and Fokurdak show rather flat REY trends (*third group*; Table 5). In both cases, the mixing with influent, oxygen-rich water yields Eh values between +200 and +300 mV. Different from these trends is that of the REY pattern of the spring water from the local travertine ridge (Eh about +60 mV). The positive Y anomalies indicate intensive water–rock interaction. The waters from the travertine ridge follow the trends of Kizildere waters but with a negative Eu anomaly. In contrast, the REY patterns of water from the Kula exploration well are typical for those having been in contact with basalts (Paces et al., 2002).

The *fourth group* (Table 5) comprises the spring waters of Pamukkale and the bottled mineral water from Kula (Fig. 7d). The REY patterns of the Pamukkale waters are very similar, more or less horizontal with strongly negative Ce, small negative Eu, and significantly positive Y anomalies. They only vary among the very light REE. The mineral water from Kula shows Ce and Y anomalies similar to the Pamukkale water but with increasing normalised concentrations from La to Lu. These patterns are typical for oxygen-rich karst waters (Möller, 2002).

3.5. Pb isotope ratios

Pb contents in the possible source rocks vary between 1 and 15 μg/g (Table 3). Between 80% and about 50% of the total Pb are leachable within 20 h from gneisses and schists, respectively (Table 4). The least fractions are leachable from shales under the applied acidic conditions. The limestones are poor in Pb (<2 ppm) and Pb is released proportional to carbonate dissolution. With exception of the well and travertine water from Kula and the hotel spring in Pamukkale, the $^{206}Pb/^{207}Pb$ ratios of the waters are all rather similar irrespective of their regional occurrences (Table 2). $^{206}Pb/^{207}Pb$ and $^{206}Pb/^{208}Pb$ ratios of some leachates are significantly higher than in

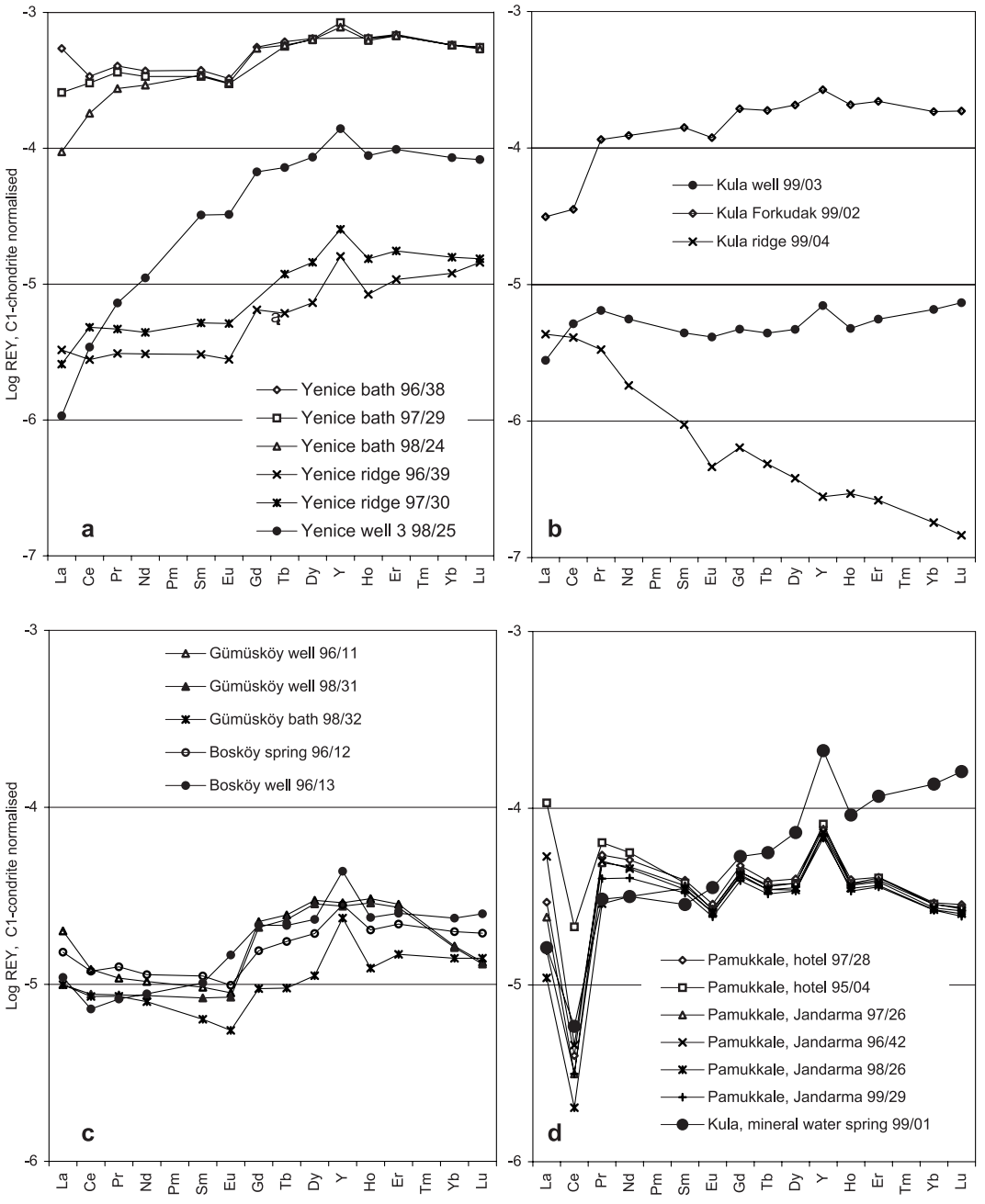

Fig. 7. C1-chondrite-normalised REY patterns of the various types of thermal spring and well waters from Yenice (a), Kula (b), Gümüsköy and Bosköy (c), and Pamukkale and Kula bottling plant (d).

waters (Table 6) and sometimes they either decrease or increase with leaching time (Table 4). These changes in isotopic composition are due to contributions from a variety of minerals of the rocks. The averages of $^{206}Pb/^{207}Pb$ and $^{206}Pb/^{208}Pb$ ratios of the waters correspond with those in leachates from the

Table 5
Grouping of the high-temperature (>100 °C) and thermal waters (<100 °C) according to their REY patterns in Figs 6 and 7

Group of REY patterns	Localities	Remarks
1	Kizildere, Salavatli, Gemencik, Salihli Tekkehamam, Babacik, Ujuzhamami, Gölemezli, Sazliköy	High-temperature waters (T>100 °C) of geothermal fields with CO_2-rich artesian wells; thermal spring- and well waters (<100 °C) in the above geothermal fields
2	Yenice, Bosköy, Gümüsköy	Thermal springs and wells (T<100 °C)
3	Kula	Hot pool Forkudak and spring on travertine ridge (T<100 °C)
4	Pamukkale, Kula	Springs feeding the travertine terraces; Well at bottling plant of mineral water

schist + marble and the Tertiary rocks, but definitely not with those of gneisses (Table 6). The Pb isotope ratios of leachates are slightly higher than those of the waters from the mica schists. This is explicable when considering the different history of ^{206}Pb and ^{207}Pb isotopes as the final daughters of the two uranium decay series. The high recoil energy of the α particles from the decay of ^{234}U (ultimately yielding ^{206}Pb) destructs the site of the radioactive daughter products (Fleischer and Raabe, 1978a,b). Thus, the daughter products including ^{206}Pb are more leached from mineral surfaces than ^{207}Pb, the end product of the ^{235}U series. In the long run, waters from such aquifers become slightly depleted in ^{206}Pb (Osmond and Cowart, 1976; Osmond et al., 1983).

4. Discussion

The REY are intimately associated with Ca in minerals and, therefore, REY patterns in CO_2 rich geothermal waters display many facets of temperature- and pressure-dependencies of carbonate equilibria. Carbonate dissolution is enhanced by high CO_2 pressures but at constant P_{CO_2}, calcite solubility decreases with increasing temperature. Dissociation constants of carbonic acid and ion activity products of both calcite and aragonite also decrease with increasing temperature, and Henry's law constant passes a maximum at about 170 °C at which the mole fraction of CO_2 dissolved in the liquid is at minimum (Fournier, 1985). CO_2 solubility is lowered with increasing salinity (Ellis and Golding, 1963). With decreasing temperature and total pressure, CO_2 exsolves during ascent and, consequently, carbonates precipitate and pH increases slightly. Some of the secondary carbonate may even be re-dissolved, if the temperature of the geothermal system decreases with time. Thus in CO_2-rich geothermal fluids, REY abundance is mainly controlled by their release from host minerals, coprecipitation with carbonates as a

Table 6
Compilation of averaged Pb isotope ratios of whole rocks and their leachates after 20 h (Table 4) and high-temperature waters (>100 °C) from geothermal fields, thermal springs and Pamukkale

	Gneiss		Mica schist + marble		Tertiary rocks	
	Whole rock	Leachate	Whole rock	Leachate	Whole rock	Leachate
Number of samples	2	4	3	6	2	4
Pb (206/208)	0.862	0.621	0.477	0.478	0.549	0.476
Pb (207/208)	0.391	0.383	0.395	0.398	0.382	0.395
Pb (206/207)	2.202	1.622	1.209	1.201	1.437	1.205
			Waters from		Thermal water from Pamukkale	
			geothermal fields	springs and wells		
Number of samples			32	25	6	
Pb (206/208)			0.473	0.468	0.473	
Pb (207/208)			0.410	0.407	0.402	
Pb (206/207)			1.154	1.150	1.179	

response of CO_2 exsolution, and surface complexation at oxihydroxides.

The release of REY from minerals of the source rock in the study area is enhanced by dissolved CO_2, which provides ample H^+ for ion exchange and hydrolysis of minerals of the source rocks. From experimental leaching, it is known that at pH 6, REY/Ca ratios are at least lower by three orders of magnitude than at pH 3 (Möller, 2002). Thus, at near-neutral pH, only small fractions of REY are leached. None of the REY patterns of leachates in Fig. 4 resemble the high-temperature waters (Fig. 6a) but these patterns show that long-term leaching preferentially depletes HREY in schists or the light to medium ones in gneisses and shales. If a steady state is established in fluid–rock interaction, the REY patterns of the waters must resemble those of the source rocks (Möller et al., 2003). Indeed, the trends of REY patterns of the schists (Fig. 3a) and the high-temperature waters (Fig. 6a) are similar and both show negative Eu anomalies.

Applying the PHREEQC program (Parkhust and Appelo, 1999) to the average Kizildere water, the REY speciation is estimated at the bottom hole conditions of 210 °C and 39 bar CO_2. About 60% of each individual REY is present as sulphate-, 20% as bicarbonate-, and 2–3% as di-sulphate and carbonate complexes, and 10–20% as free ions. In spite of the high CO_2 contents of the fluid, the much lower sulphate content dominates REY complexation.

The low redox potentials of the deep-seated waters in comparison with the high potentials in various springs (Yenice, Kula) proves mixing of deep-seated (H_2S bearing) and oxygen-rich groundwater. This mixing yields reduction of temperature and oxidation of dissolved Fe(II) and H_2S. The oxidised Fe forms colloids which may or may not be precipitated onto mineral surfaces along the water's pathways. The colloids could not quantitatively be separated from the water by filtration, and the sorbed REY appear as part of the acidified solutions. From the experiments, it is known that gel coagulation preferentially removes the middle to heavy REY leaving the light REE and Y in solution but with only Ce being significantly removed due to its oxidation (Bau, 1999; Kawabe et al., 1999). This type of fractionation is responsible for strongly negative Ce anomalies and enhanced Y/Ho ratios in the oxygen-rich waters of the Kula mineral water and the Pamukkale springs (Fig. 7d).

The high-temperature and thermal spring waters show Er/Ca ratios ranging from 1 to 14 ng/g. These low ratios contrast those of 100–500 ng/g in exploration wells and hot pools (Ujuzhamami, Forkurdak). Ratios in between these are exhibited by Yenice bath, Gümüsköy and Bosköy. As evident for Yenice bath, the high ratios are caused by dissolution of FeOOH colloids remaining after filtration.

The normalised REY abundance in spring waters may be enhanced ($>10^{-4}$) due to interaction of Na^+- and HCO_3^- – rich waters with clay minerals of the sediments in the presence of HCO_3^- as a chemically complexing agent (Yenice bath and Kula Forkudak in Fig. 7a and b, respectively). For instance, the spring waters of Tekkehamam, Babacik, Ujuzhamami, Gölemesli and Sazliköy (Fig. 6b) show patterns similar to those of the Kizidere well waters ($<10^{-5}$) but at enhanced REY abundances ($<10^{-4}$).

The absence of a negative Eu anomaly in local gneisses (Fig. 3a) excludes them as the REY controlling source rock of the Kizildere water. The marble can also be excluded because of its negative Ce and positive Y anomalies which are absent in Kizildere water. The Tertiary sedimentary rocks can reasonably be excluded because of the absence of a sufficient heat source at shallow depth. Thus, only the mica schists and interbedded lithologies remain as the most probable REY controlling source among the basement rocks. Thus, REY abundance of the CO_2-rich, oxygen-poor, high-flow, high-temperature water is dominantly controlled by the mica schists of the basement at about 230 °C. The water does not penetrate down into the underlying gneisses (Fig. 2). Only the CO_2 originates from below and has to pass the gneisses probably along faults (Giese, 1997). Karstic marbles of the basement and the Pliocene limestone may act as important aquifers of the thermal water. Due to carbonate saturation of the deep-seated water with Er/Ca$>10^{-8}$ (Table 2), interaction with Neogene carbonates low ratios Er/Ca$<10^{-9}$ (Table 3) with is negligible and changes the REY patterns of water only insignificantly. Furthermore, during ascent of water, carbonates precipitate upon exsolution of CO_2 and, thus, coat all surfaces. With temperatures of about 200 °C, the fractionation of REY is negligible as proved by scale formation (Fig. 3b). Furthermore, the producing wells yield water with

lower REY abundance and Y/Ho ratios than the exploration wells (Gemencik, Salavatli, Kula).

The thermal spring waters of the Kizildere area (Tekkehamam, Babacik, and Gölemezli) are directly related to a deep-seated aquifer with minor interaction with Pliocene sedimentary rocks. The Ca^{2+} contents of these waters are significantly enhanced due to dissolution of carbonates at temperatures below 100 °C. The increase in Eh values from −120 to +35 mV, enhanced Mg^{2+} and SO_4^{2-} contents (Table 2) indicate mixing with ambient groundwater before discharge. Most of the CO_2 reacts with sediments by which REY abundance in waters increase and flat patterns of heavy REE with strongly positive Y anomalies develop. Na undergoes ion exchange with clay minerals of the graben sediments.

A different type of water is represented by the shallow wells of Yenice, Kula and Bosköy and associated springs. The REY abundance of these waters is controlled by reaction with minerals of the Pliocene sediments. High CO_2 contents enable dissolution of carbonates at temperatures around 100 °C. When emerging at the surface, travertine precipitates due to exsolution of CO_2. Mixing with ambient groundwater yields Eh values between 0 and +330 mV and cooling.

The springs of Pamukkale show REY abundance in thermal water being exclusively controlled by the dissolution of carbonates by oxygen-rich waters, i.e. progress of karstification of the Neogene limestone. The heat and the CO_2 source may be the same as in the Kizildere group of waters but the meteoric water does not penetrate to the same stratigraphic depth. Therefore, the temperatures are lower. Probably, the fractures are sealed towards depth and only CO_2 passes and dissolves in the oxygen-rich water.

The Kula mineral water is not related to the Kula marble. It represents CO_2-rich groundwater which interacted with the carbonates that once formed from ascending hot waters. The REY abundance of this carbonate can be delineated from patterns of the Kula well water and the spring water from the local travertine ridge. From Fig. 7b, it is evident that this carbonate increases from La to Lu by one order of magnitude, and such an increase characterises the REY patterns of Kula mineral water.

Along deep-reaching faults, the meteoric waters penetrate down to the crystalline Palaeozoic rock units with a large regional heat source underlying the study area, probably with apophyses localised near the known geothermal fields. Only at Pamukkale the hydrologic regime is different. The main processes that occur are the interaction of the ascending CO_2 and the interaction of influent water with the local rocks and later storage in karst formations. Precipitation of carbonates due to changes in temperature and CO_2 partial pressure leads to changes in REY patterns during the ascent of water. If the precipitation is very fast and at high temperatures, the changes in REY are less than in slow precipitation processes at low temperature, when light REY become enriched in carbonates due to increased formation of bicarbonate and carbonate complexes.

5. Conclusions

The following conclusions can tentatively be drawn:

- REY can be used to decipher the source rock or sediment in which the final REY patterns are controlled. This is the unit which releases the highest amounts of REY during water–rock interaction. In systems active over geological times, the REY abundance in surfaces or coatings of minerals along the flow path in subsequent rock units is adjusted to that of the passing waters which leads to only insignificant changes of REY in percolating water. In this way, REY allow insight behind the aquifers which largely control the macrochemistry of the thermal waters.
- REY abundance is much higher in thermal water from closed exploration wells than from production wells because of the different steady states.
- REY allow distinction between stationary and non-stationary water–rock interaction, which is mainly expressed by the presence or absence of both Eu and Y anomalies in the REY patterns.
- Negative Ce anomalies indicate FeOOH precipitation along the pathway of infiltrating waters.
- Spring and well waters in a geothermal field related to the deep-seated, high-temperature source show

significantly different REY patterns compared with those of waters from shallow aquifers. Such REY patterns are not exclusively controlled by faults but also depend on local infiltration of meteoric water and the location of the heat source.

Acknowledgements

The authors thank E. Oelkers, D. Banks and J.R. Haas for their critical comments. The help of N. özgür in organising the field trips and the analytical assistance of B. Richert, C. Wiesenberg and B. Zander are gratefully acknowledged. **[EO]**

References

Aggarwal, J., Shabani, M.B., Palmer, M.R., Ragnarsdottir, K.V., 1996. Determination of the rare earth elements in aqueous samples at sub-ppt levels by inductively coupled plasma mass spectrometry and flow injection ICPMS. Anal. Chem. 68, 4418–4423.

Bau, M., 1999. Scavenging of dissolved yttrium and rare earths by precipitating iron oxyhydroxides: experimental evidence for Ce oxidation, Y–Ho fractionation, and lanthanide tetrad effect. Geochim. Cosmochim. Acta 63, 67–77.

Bau, M., Dulski, P., 1996. Anthropogenic origin of positive gadolinium anomalies in river waters. Earth Planet. Sci. Lett. 143, 245–256.

Bau, M., Möller, P., 1992. Rare earth fractionation in metamorphic hydrothermal calcite, magnesite and siderite. J. Mineral. Petrol. 45, 231–246.

Bilal, B.A., 1991. Thermodynamic study of Eu^{3+}/Eu^{2+} redox reaction in aqueous solutions at elevated temperatures and pressures by means of cyclic voltammetry. Z. Naturforsch. 46a, 1108–1116.

Doglioni, C., Agostini, S., Crespi, M., Innocenti, F., Manetti, P., Riguzzi, F., Savascin, M.Y., 2002. On the extension in western Anatolia and the Agean Sea. J. Virtual Explor. 8, 169–183.

Dulski, P., 1994. Interferences of oxide, hydroxide and chloride analyte species in the determination of rare earth elements in geological samples by inductively coupled plasma-mass spectrometry. Fresenius' J. Anal. Chem. 350, 194–203.

Dulski, P., 2001. Reference materials for geochemical studies: new analytical data by ICP-MS and critical discussion of reference values. Geostand. Newsl. 25, 87–125.

Ellis, A.J., Golding, R.M., 1963. The solubility of carbon dioxide above 100 °C in water and in sodium chloride solutions. Am. J. Sci. 261, 1323–1357.

Erdogan, B., Güngor, T., 1992. Menderes Masifinin Kuzey Kanadinin Stratigrafisi ve Tektonik Evrimi. Turk. Assoc. Petrol. Geol. Bull. 4, 9–34.

Fleischer, R.L., Raabe, O., 1978a. Recoiling alpha emitting nuclei. Mechanisms for uranium series disequilibrium. Geochim. Cosmochim. Acta 42, 973–978.

Fleischer, R.L., Raabe, O., 1978b. Recoiling alpha emitting nuclei. Mechanisms for uranium series disequilibrium. Geochim. Cosmochim. Acta 42, 973–978.

Fournier, R.O., 1985. Carbonate transport and deposition in the epithermal environment. In: Berger, B.R., Bethke, P.M. (Eds.), Geology and Geochemistry of Epithermal Systems. Reviews in Economic Geology, vol. 2, pp. 63–72.

Francalanci, L., Innocenti, F., Manetti, P., Savascin, M.Y., 2000. Neogene alkaline volcanism of the Afyon–Isparta area, Turkey: petrogenesis and geodynamic implications. J. Mineral. Petrol. 70, 285–312.

Giese, L., 1997. Geothechnische und umweltgeologische Aspekte bei der Förderung und Reinjektion von Thermalfluiden zur Nutzung geothermischer Energie am Beispiel des Geothermalfeldes Kizildere und des Umfeldes, W-Anatolien/Türkei. PhD thesis. Free University Berlin. 220 pp.

Giese, U., Bau, M., 1994. Trace element accessibility in mid-ocean ridge and ocean island basalt: an experimental approach. Mineral. Mag. 58A, 329–330.

Honda, T., Oi, T., Ossaka, T., Nozaki, T., Kakihana, H., 1989a. Determination of rare earth elements in hot spring and crater lake waters by epithermal neutron activation analysis. J. Radioanal. Nucl. Chem. 133, 301–315.

Honda, T., Oi, T., Ossaka, T., Nozaki, T., Kakihana, H., 1989b. Determination of praseodymium, neodymium and erbium in hot spring and crater lake waters by neutron activation analysis incorporating the standard addition technique. J. Radioanal. Nucl. Chem. 134, 13–25.

Innocenti, F., Agostini, S., Di Vinzenzo, G., Doglioni, C., Manetti, P., Savascin, M.Y., Tonarini, S., in press. Neogene and Quaternary volcanism in Western Anatolia: magma sources and geodynamic evolution. Marine Geology, Special Issue Eastern Mediterranean.

Irber, W., 1996. Laugungsexperimente an peraluminischen Graniten als Sonde für Alterationsprozesse im finalen Stadium der Granitkristallisation mit Anwendung auf das Rb–Sr–Isotopensystem. PhD thesis. Free University Berlin. 319 pp.

James, R.H., Elderfield, H., Palmer, M.R., 1995. The chemistry of hydrothermal fluids from the Broken Spur site, 29°N Mid-Atlantic Ridge. Geochim. Cosmochim. Acta 59, 651–659.

Kawabe, I., Ohta, A., Miura, N., 1999. Distribution coefficients of REE between Fe oxyhydroxide precipitates and NaCl solutions affected by REE-carbonate complexation. Geochem. J. 33, 181–197.

Kikawada, Y., Oi, T., Honda, T., Ossaka, T., Kakihana, H., 1993. Lanthanoid abundances of acidic hot spring and crater lake waters in the Kusatsu-shirane volcano region. Jpn. J. Geochem. 27, 19–33.

Klinkhammer, G.P., Elderfield, H., Edmond, J.M., Mitra, A., 1994. Geochemical implications of rare earth element patterns in hydrothermal fluids from mid-ocean ridges. Geochim. Cosmochim. Acta 58, 5105–5113.

Langelier, W., Ludwig, H., 1942. Graphical methods for indicating the mineral character of natural waters. J. Am. Water Assoc. 34, 335–352.

Lepel, E.A., Laul, J.C., Smith, M.R., 1989. Rare earth element patterns in briny groundwaters (analog study). Radioact. Waste Manag. Nucl. Fuel Cyle 13, 367–377.

Lewis, A.J., Komninou, A., Yardley, B.W.D., Palmer, M.R., 1998. Rare earth speciation in geothermal fluids from Yellowstone National Park, Wyoming, USA. Geochim. Cosmochim. Acta 62, 657–663.

Michard, A., 1989. Rare earth systematics in hydrothermal fluids. Geochim. Cosmochim. Acta 53, 745–750.

Michard, A., Albarede, F., 1986. The REE contents of some hydrothermal fluids. Chem. Geol. 55, 51–60.

Michard, A., Michard, G., Stüben, D., Stoffers, P., Cheminee, J.-L., Binard, N., 1993. Submarine thermal springs associated with young volcanoes: the Teahitia vents, Society Island, Pacific Ocean. Geochim. Cosmochim. Acta 57, 4977–4986.

Middlesworth, P.E., Wood, S.A., 1998. The aqueous geochemistry of the rare earth elements and yttrium: Part 7. REE, Th and U contents in thermal springs associated with the Idaho batholith. J. Appl. Geochem. 13, 861–884.

Möller, P., 1998. Rare earth elements and yttrium fractionation caused by fluid migration. In: Novak, M., Rosenbaum, J. (Eds.), Challenges to Chemical Geology. Czech Geological Survey (Prague), pp. 9–32.

Möller, P., 2000. Rare earth elements and yttrium as geochemical indicators of the source of mineral and thermal waters. In: Stober, I., Bucher, K. (Eds.), Hydrogeology of Crystalline Rocks. Kluwer Academic Publishing, Dodrecht, Netherlands, pp. 227–246.

Möller, P., 2002. Rare earth elements and yttrium distribution in water–rock interactions: field observations and experiments. In: Stober, I., Bucher, K. (Eds.), Water–Rock Interaction. Kluwer Academic Publishing, Dordrecht, The Netherlands, pp. 97–123.

Möller, P., Giese, U., 1997. Determination of easily accessible metal fractions in rocks by batch leaching with acid cation-exchange resin. Chem. Geol. 137, 41–55.

Möller, P., Morteani, G., Hoefs, J., 1985. REE and 18O/16O distribution in altered Variscan granites of the western Harz, Germany and southern Sardinia, Italy. High Heat Production (HHP) Granites, Hydrothermal Circulation and Ore Genesis. The Institute of Mining and Metallurgy, London, UK, pp. 213–220.

Möller, P., Dulski, P., Gerstenberger, H., Morteani, G., Fuganti, A., 1998. Rare earth elements, yttrium and H, O, C, Sr, Nd and Pb isotope studies in mineral waters and corresponding rocks from NW Bohemia Czech Republic. Appl. Geochem. 13, 975–994.

Möller, P., Dulski, P., Morteani, G., 2003. Partitioning of rare earth elements, yttrium, and some major elements among source rocks, liquid and steam of Larderello–Travale Geothermal Field, Tuscany (Central Italy). Geochim. Cosmochim. Acta 67, 171–183.

Okay, A.I., Siyako, M., Burkan, K.A., 1991. Geology and tectonic evolution of the Biga Peninsula, northwest Turkey. Bull. Tech. Univ. Istanb. 44, 191–256.

Osmond, J.K., Cowart, J.B., 1976. The theory and uses of natural uranium isotope variations in hydrology. At. Energy Rev. 14, 621–679.

Osmond, J.K., Cowart, J.B., Ivanovich, M., 1983. Uranium isotope disequilibrium in groundwater as an indicator of anomalies. Int. J. Appl. Radiat. Isot. 34, 283–308.

Paces, T., Möller, P., Fuganti, A., Morteani, G., Pecek, J., 2002. Sparkling mineral water at western rim of the Doupovske hory Mountains (Czech Republic): genesis by water–rock interaction and deep-seated CO_2. Bull. Czech Geol. Surv. 76, 189–202.

Parekh, P.P., Möller, P., Dulski, P., 1977. Distribution of trace elements between carbonate and non-carbonate phases of limestone. Earth Planet. Sci. Lett. 34, 39–50.

Parkhust, D.L., Appelo, C.A.J., 1999. User's Guide to PHREEQC (Version 2). A computer program for speciation, batch-reaction, one-dimensional transport, and inverse geochemical calculations. Water-Resources Investigation Report. U.S. Geol. Surv., Denver, pp. 99–4259.

Satman, A., Ugur, Z., Onur, M., 1999. The effect of calcite deposition on geothermal well inflow performance. Geothermics 28, 425–444.

Sengör, A.M.C., 1979. The North Anatolian transform fault; its age, offset and tectonic significance. J. Geol. Soc. (Lond.) 136, 269–282.

Sverjensky, D.A., 1984. Europium redox equilibria in aqueous solution. Earth Planet. Sci. Lett. 67, 70–78.